[30]P. G. Burke, Advan. Phys. 14, 521 (1965).

[31]W. Lichten, Phys. Rev. 131, 229 (1963).

[32]R. J. Eden and J. R. Taylor, Phys. Rev. Letters 11, 516 (1963); Phys. Rev. 133, B1575 (1964); M. Ross, Phys. Rev. Letters 11, 450 (1963). D. Amatc, Phys. Letters 7, 290 (1963); N. Nauenberg and J. C. Nearing, Phys. Rev. Letters 12, 63 (1964); R. H. Dalitz and G. Rajasckaran, Phys. Letters 7, 373 (1963).

[33]All complex poles in the S matrix at energy Ep are accompanied by poles at $E_p{}^*$ but this is not the multiplicity referred to here.

PHYSICAL REVIEW VOLUME 174, NUMBER 1 5 OCTOBER 1968

Diffusion of He (2^3S_1) in Helium Gas; $2^3S_1 - 1^1S_0$ Interaction Potentials at Long Range*

W. A. Fitzsimmons, N. F. Lane,† and G. K. Walters

Department of Physics, Rice University, Houston, Texas

(Received 6 May 1968)

The existence at intermediate separations of a repulsive barrier in the interaction potentials between a He(2^3S_1) metastable atom and a He(1^1S_0) ground-state atom has been well established both experimentally and theoretically. The present investigation deals with the quantitative nature of this repulsive interaction for large internuclear separations. The diffusion coefficient, and thus the diffusion cross section, for He(2^3S_1) atoms in helium gas has been measured over the temperature range from 1 to 300°K by means of a pulsed afterglow technique. The diffusion cross sections so determined are 82, 58, 46, and 34 (10^{-16} cm^2) ±5% at 4.2, 20, 77, and 300°K, respectively. For purposes of comparison, diffusion cross sections were also calculated quantum mechanically using adjustable long-range potentials of a form consistent with previous theoretical calculations. A comparison of the calculated and measured diffusion cross sections clearly indicates that the previous theoretically determined interaction potentials are much too strongly repulsive at large internuclear separations. Accordingly the parameters in the adjustable potentials were varied until agreement with the experimental diffusion cross sections was obtained. The adjusted interaction potentials were then used to calculate total and excitation transfer cross sections, and the results are shown to be in excellent agreement with previous and independent experimental measurements.

I. INTRODUCTION

The interaction potentials between helium atoms in the excited 2^3S_1 state and the 1^1S_0 ground state have been the subject of considerable theoretical and experimental investigation.[1–6] The interest in this interaction stems from the fact that both the $^3\Sigma_u{}^+$ and the $^3\Sigma_g{}^+$ molecular potential functions, though attractive at shorter range, exhibit repulsive barriers at intermediate nuclear separations.

This behavior was first established theoretically for the $^3\Sigma_u{}^+$ state by Buckingham and Dalgarno.[1] Their calculations indicated a binding minimum for an internuclear separation R of about $2a_0$, and a repulsive maximum at $R = 4a_0$ with a barrier height of 0.29 eV. These authors pointed out that the presence of the barrier would have the effect of reducing the diffusion coefficient of 2^3S_1 atoms at low temperatures, and would lead to a $2^3S_1 - 1^1S_0$ excitation-transfer cross section which falls off rapidly at low (thermal) energies in contrast to the behavior expected for attractive interactions.

More sophisticated theoretical calculations of the $^3\Sigma_{g,u}^+$ molecular potentials in helium were undertaken by Matsen and co-workers.[2–4] These calculations were intended to reconfirm the theoretical basis of the repulsive interaction and to accurately determine the interaction energies in the region of the potential maxima and minima. Their results have shown that both the $^3\Sigma_u^+$ and the $^3\Sigma_g^+$ interactions tions have attractive minima near $2a_0$ with repulsive barriers in the neighborhood of $4.5a_0$. The predicted barrier heights have tended to decrease slightly as these calculations were improved, the latest estimate of the $^3\Sigma_u$ barrier height being about eV.[2,4]

Strong experimental evidence for the existence of the barrier was provided by Colegrove, Schearer, and Walters.[5] They used an optical pumping technique on discharge-excited He^3 to study excitation transfer in 2^3S_1-1^1S_0 collisions and found the reaction rate to fall off rapidly with decreasing temperature below 300°K. This was in qualitative agreement with the predictions of Buckingham and Dalgarno,[6] though the measured rates were substantially larger than had been predicted.

The present investigation was undertaken in order to determine the long-range interaction appropriate to the calculation of cross sections at thermal energies. The experimental study consisted of measuring the diffusion coefficient for triplet metastable helium atoms in helium gas over the tempera-

ture range of 1 to 300°K. Diffusion cross sections were extracted from the experimental data by use of the Chapman-Enskog relation, and the results were compared with diffusion cross sections calculated using the best available theoretical potentials.[4] The agreement obtained was poor; therefore the long-range portions of the interaction potentials were parametrized in a manner consistent with the previous theoretical calculations, and the parameters varied until the calculated and experimentally determined diffusion cross sections were in good agreement. Finally, the long-range repulsive interaction determined on the basis of the diffusion data was used to calculate total and excitation transfer cross sections, and the results were found to be in excellent agreement with previous and independent experimental measurements.

II. EXPERIMENTAL PROCEDURE

A conventional discharge afterglow technique was used to measure the temperature dependence of the diffusion coefficient of metastable 2^3S_1 helium atoms in helium gas. At low helium densities, the average lifetime of atoms in the 2^3S_1 state is determined by diffusion to the container walls where de-excitation occurs.

Helium samples were contained in carefully prepared spherical Pyrex vessels approximately 5 cm in diameter. After thorough electrical-discharge cleaning, the vessels were filled with helium gas to the desired densities through a liquid-helium labyrinth trap, and then tipped off to yield permanently sealed samples of high purity.

The experimental arrangement is shown in Fig. 1. The sample is immersed in a cryogenic fluid inside the inner Dewar flask, and its temperature is determined by measuring the fluid vapor pressure. Sample temperatures ranging from 1.0 to 300°K

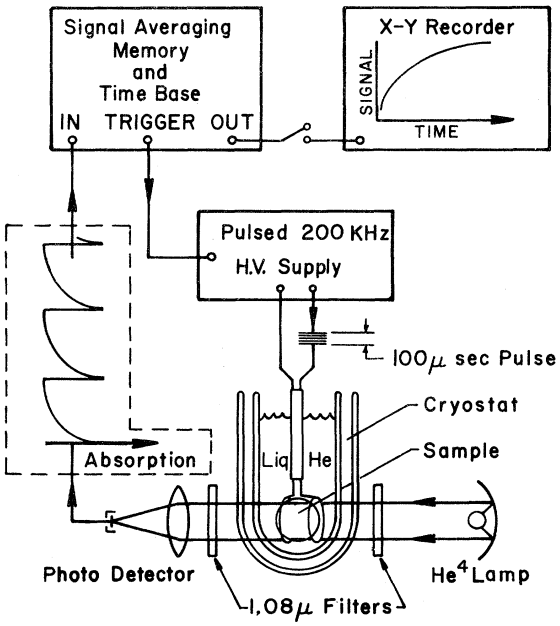

FIG. 1. Schematic diagram of apparatus used in $He(2^3S_1)$ diffusion measurements.

are achieved by using helium, hydrogen, nitrogen, and Freon-12 liquids as coolants.

Metastable lifetime measurements are initiated by periodically igniting a weak electrodeless 200-kHz electrical discharge in the sample. The rf pulse is typically 100-μsec long and is of sufficient intensity to provide a 2^3S_1 population of about 5×10^9 to $1\times10^{10}/cm^3$. Pulse repetition rates of 2 to 250 per second are used depending on sample density and temperature. The 2^3S_1 population is monitored during the pulse afterglow period by measuring the absorption of 10 830-Å (2^3S-2^3P) resonance radiation, for which purpose the Dewar flasks are strip silvered. The silicon-photodiode detector circuit has a response time of 60 μsec. The periodic absorption signal is averaged over many cycles by a Princeton Applied Research wave form eductor and is recorded on an X-Y plotter.

Metastable lifetimes are extracted from a semilog plot of the 2^3S_1 population versus time in the very late afterglow period. By then, conversion of singlet 2^1S_0 metastable to the 2^3S_1 state is complete,[7] and the 2^3S_1 population is governed by lowest-mode diffusion to the container walls. Figure 2 is a log plot of representative lifetime data, showing the single-exponential 2^3S_1 decay in the late afterglow period. The 2^3S_1 diffusion coefficient D is calculated from the decay time constant τ assuming the lowest diffusion mode. For our 5-cm-diam sample containers, the diffusion length is $\Lambda_1 = 0.78$ cm so that $D = \Lambda_1^2/\tau = 0.61\tau^{-1}$ cm^2/sec. This expression for D assumes unit probability for $He(2^3S_1)$ de-excitation upon collision with the container wall. Following the method of McCoubrey,[8] it was established that the effects of reflections of 2^3S_1 atoms at the container wall are negligible over the range of helium densities and temperatures used in these experiments.

Considerable care was taken to be sure that discharge pulsing did not heat the sample gas significantly. That this was not the case was established in two independent ways. First, the energy input per pulse was determined at 4.2°K by measuring the increase in the liquid-helium boil-off rate when a continuous discharge was ignited in the sample. Under typical experimental conditions the total power input to the discharge is about 5mW, but it increases rapidly at higher discharge levels. (It is of course for this reason that particularly weak pulsed discharges are employed, yielding the quoted very low 2^3S_1 concentrations.) A 5-mW 100-μsec pulse can raise the sample temperature by no more than 10^{-2}°K. Since adequate thermalization time elapses between pulses, it is safe to assume that the sample temperature is indeed equal to that of the coolant in which it is immersed.

In a second test for heating effects, the characteristic 2^3S_1 afterglow decay time was measured as a function of discharge pulse energy. No dependence of τ on pulse energy was observed until the energy was increased by more than a factor of 10 above the value used in the experiment.

III. EXPERIMENTAL RESULTS

The quantity $D\rho$ (cm^2/sec)$\times$(density, in units corresponding to a pressure of 1 Torr at 300°K) is

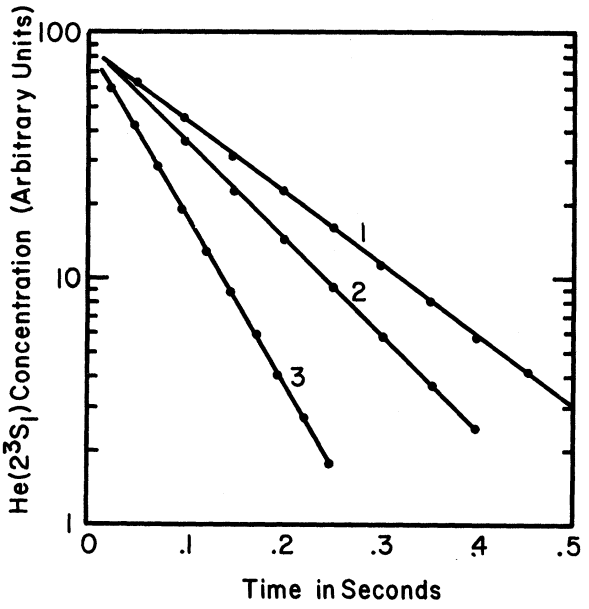

FIG. 2. Representative He(2^3S_1) lifetime data in the late afterglow of the pulsed discharge. Curves 1–3 correspond to measurements at 1.0, 2.0, and 4.2°K, respectively, with sample density corresponding to a pressure of 2.5 Torr at 300°K.

shown as a function of temperature in Fig. 3; the inset shows the low-temperature data with an expanded temperature scale. The product $D\rho$ is constant to within ±5% at liquid-helium temperatures for a range of sample densities corresponding to pressures between 0.57 and 2.5 Torr at 300°K. This confirms that diffusion to the walls is in fact the observed metastable loss mechanism. The uncertainty in $D\rho$ at all temperatures is estimated to be ±5%.

The result at 300°K, $D\rho = 480 \pm 25$ (cm²/sec) Torr, is in good agreement with the early measurements of Phelps.[7] However, the results at liquid-helium temperatures are in gross disagreement with the values reported by Fugol and Pakhomov.[9] They have reported an anomalously large 2^3S_1 diffusion coefficient measured by techniques similar to ours. We believe their measurements to be in error, perhaps because of sample heating or because their data were taken too early in the afterglow period.

The Chapman-Enskog theory relates the diffusion coefficient D to the average diffusion cross sections $\bar{Q}_D(T)$,[10]

$$D = 3kT/16\mu N\Omega_D , \tag{1}$$

where Ω_D is the diffusion collision integral

$$\Omega_D = (kT/2\pi\mu)^{1/2}\bar{Q}_D(T)$$

with

$$\bar{Q}_D(T) = \int_0^\infty e^{-g^2} Q_D(v) g^5 dg. \tag{2}$$

Here $g = (\mu v^2/2kT)^{1/2}$, k is Boltzmann's constant, T the absolute temperature, μ the reduced mass or twice the proton mass, N the gas density in atoms/cm³, and v the relative velocity in cm/sec. The averaged diffusion cross section $\bar{Q}_D(T)$ will be the point of comparison between the experimental results shown in Fig. 3 and the corresponding calculated values discussed in the next section.

IV. THEORY

The quantum-mechanical treatment of collisions between atoms having identical nuclei has been given by Massey and Smith.[11] They employed the standard adiabatic approximation in which the electronic problem is solved first for all fixed internuclear separations. The relative nuclear motion is then determined by the electronic energies plus the nuclear Coulomb repulsion. The two electronic states arising from the separated He(2^3S_1) and He(1^1S_0) atoms are the lowest $^3\Sigma_g^+$ and $^3\Sigma_u^+$ states of He_2. We denote the respective electronic wave functions by $\chi(^3\Sigma_g)$ and $\chi(^3\Sigma_u)$ and potential energies (including nuclear replusion) by $V_+(R)$ and $V_-(R)$, where R designates the relative positions

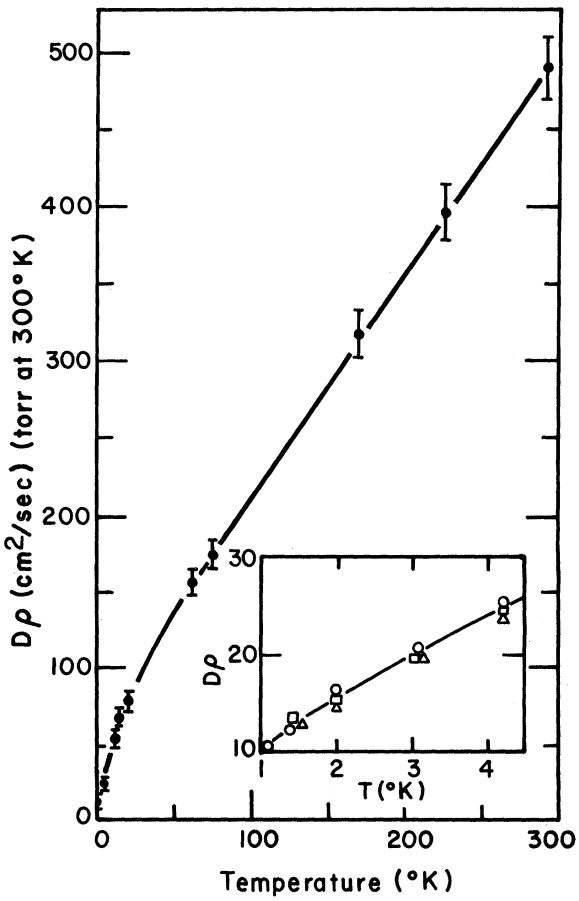

FIG. 3. Product of He(2^3S_1) diffusion coefficient and helium-gas density versus temperature. The circular, square, and triangular points correspond to helium-gas densities of 2.5, 1.5, and 0.57 Torr at 300°K, respectively.

of the nuclei. In the case of $He^4(^3S)$-$He^4(^1S)$ scattering, the total wave function must be symmetric with respect to interchange of the nuclei and, in this two-state approximation, the total wave function takes the form

$$\psi^+(\vec{R}) = \Phi(\vec{R}) + \Phi(-\vec{R}), \tag{3}$$

where

$$\Phi(\vec{R}) = \chi(^3\Sigma_g)F_+(\vec{R}) + \chi(^3\Sigma_u)F_-(\vec{R}),$$

in which $F_+(\vec{R})$ and $F_-(\vec{R})$ represent the relative motion of the nuclei and, in the adiabatic approximation, are solutions of the following uncoupled differential equations (atomic units are used throughout):

$$\nabla_{\vec{R}}^2 F_+(\vec{R}) + [k^2 - (2\mu/m)V_+(R)]F_+(\vec{R}) = 0,$$

$$\nabla_{\vec{R}}^2 F_-(\vec{R}) + [k^2 - (2\mu/m)V_-(R)]F_-(\vec{R}) = 0, \tag{4}$$

where $\nabla_{\vec{R}}^2$ is the Laplacian operator in the relative nuclear coordinate $\vec{R}$, μ is the reduced mass of the helium nuclei, m is the mass of the electron, and $k/a_0 = \mu v/\hbar$, where v is the relative velocity. The solutions of Eqs. (4) represent the scattering process and for large R have the asymptotic form

$$F_\pm(\vec{R}) = \alpha_\pm[e^{ikZ} + R^{-1}e^{ikR}f_\pm(\theta)]. \tag{5}$$

The coefficients $\alpha_\pm$ are determined by requiring that the incident $He(2^3S_1)$ atoms be described by a plane wave of unit amplitude moving in the positive Z direction; θ is the center-of-mass scattering angle. The resulting asymptotic expression for the total wave function $\psi^+(\vec{R})$ yields the total scattering amplitude

$$f(\theta) = \tfrac{1}{2}[f_+(\theta) + f_+(\pi-\theta) + f_-(\theta) - f_-(\pi-\theta)]. \tag{6}$$

The partial scattering amplitudes $f_\pm(\theta)$ can be expressed in terms of the scattering phase shifts η_L^+ and η_L^- appropriate to the interaction potentials $V_+(R)$ and $V_-(R)$, respectively:

$$f_\pm(\theta) = (2ik)^{-1}\sum_{L=0}^{\infty}(2L+1) \times (\exp 2i\eta_L^{\pm} - 1)P_L(\cos\theta). \tag{7}$$

The total and diffusion cross sections are given by

$$Q_{\text{tot}} = 2\pi\int_0^\pi |f(\theta)|^2 \sin\theta d\theta = (4\pi/k^2)\sum_L (2L+1)\sin^2\delta_L, \tag{8}$$

$$Q_D = 2\pi\int_0^\pi |f(\theta)|^2(1-\cos\theta)\sin\theta d\theta = (4\pi/k^2)\sum_{L=0}^{\infty}(L+1)\sin^2(\delta_{L+1} - \delta_L), \tag{9}$$

where $\delta_L = \eta_L^+$, $\delta_{L+1} = \eta_{L+1}^-$, L_{even};

$\delta_L = \eta_L^-$, $\delta_{L+1} = \eta_{L+1}^+$, L_{odd}.

Equations (8) and (9) include the effects of nuclear symmetry.

At higher energies, where the amplitudes $f_+(\theta)$ and $f_-(\theta)$ are strongly peaked in the forward direction, the cross terms in the scattering intensity may be neglected and $|f(\theta)|^2$ takes on the following form independent of nuclear symmetry:

$$|f(\theta)|^2 = \tfrac{1}{4}\{|f_+(\theta) + f_-(\theta)|^2 + |f_+(\pi-\theta) - f_-(\pi-\theta)|^2\}. \tag{10}$$

The first term on the right-hand side of Eq. (10) is interpreted as the direct elastic scattering of the incident metastable atoms from the ground-state atoms. By analogy with nonresonance transfer collisions, the second term or large-angle contribution to the scattering intensity is interpreted as being due to the transfer of excitation between the projectile and target atoms. The second term, when integrated over all angles, is the excitation-transfer cross section:[12]

$$Q_{\text{trans}} = (\pi/k^2)\sum_{L=0}^{\infty}(2L+1)\sin^2(\eta_L^+ - \eta_L^-). \tag{11}$$

In this approximation we may write

$$Q_{\text{tot}} = Q_{\text{el}} + Q_{\text{trans}},$$

where

$$Q_{\text{tot}} = (2\pi/k^2)\sum_{L=0}^{\infty}(2L+1)(\sin^2\eta_L^+ + \sin^2\eta_L^-). \tag{12}$$

The diffusion cross section takes on the slightly simpler form

$$Q_D = (2\pi/k^2)\sum_{L=0}^{\infty}(L+1)[\sin^2(\eta_L^+ - \eta_{L+1}^-) + \sin^2(\eta_{L+1}^+ - \eta_L^-)]. \tag{13}$$

Calculation of the scattering phase shifts $\eta_L^\pm$ and thus the cross sections is straightforward provided the interaction potentials $V_+(R)$ and $V_-(R)$ are known. We have calculated cross sections Q_{tot} and Q_D both from Eqs. (8) and (9) and also from the simpler Eqs. (12) and (13); the differences were found to be negligible for energies greater than 10^{-3} eV.

The most recent published theoretical calculations of the $He(2^3S)$-$He(1^1S)$ interaction potentials were carried out by Matsen and Scott[2] ($^3\Sigma_u^+$) and Greenawalt[3] ($^3\Sigma_g^+$) and adjusted in a semiempirical manner by Klein, Greenawalt, and Matsen.[4] These curves are illustrated in Fig. 4. The respective heights and positions of the repulsive barriers are 0.36 eV at $3.5a_0$ for $V_+(R)$ and 0.16 eV at $4.5a_0$ for $V_-(R)$. More recent calculations indicate the barriers to be somewhat lower.[13] In the calculation of the $^3\Sigma_g^+$ energy, Greenawalt[3] and Matsen employed both a five- and a 50-term variational function. The two resulting $V_+(R)$ curves differ markedly in that the five-term curve crosses the $V_-(R)$ curve of Matsen and Scott at about $7a_0$ while the 50-term curve remains above $V_-(R)$ for all R. The 50 term $V_+(R)$, however, seems to remain

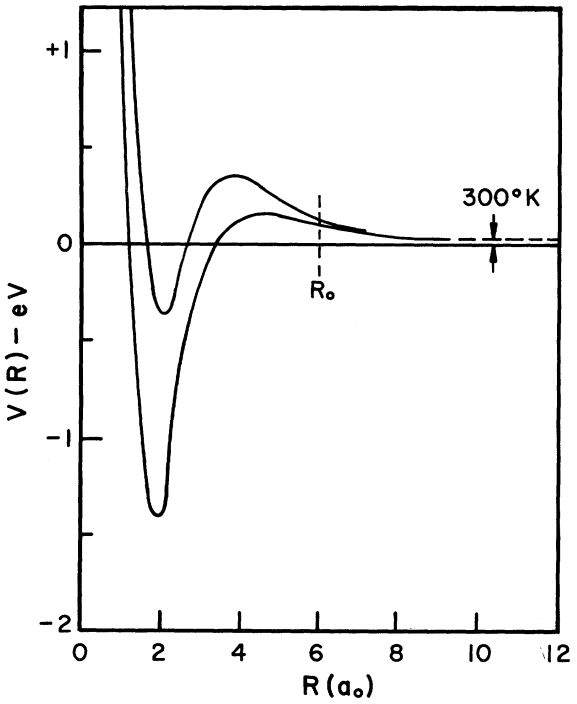

FIG. 4. Theoretically predicted He(2^3S_1)-He(1^1S_0) interaction potentials as calculated by Matsen and Scott (V_-) and Greenawalt (V_+) and adjusted semi-empirically by Klein, Greenawalt, and Matsen (Refs. 2-4). (Refs. 2-4).

too large at large separations. Our procedure in this work is to accept the short-range portions of the interaction potential $V_-(R)$ calculated by Matsen and Scott and the five-term results for $V_+(R)$ of Greenawalt.[3] Simple analytic forms are chosen to represent these potentials in the region $R \leq R_0$, where $R_0 = 6a_0$ was found to be convenient. Because of the existence of rather high and broad barriers in both potentials, calculated cross sections for the energies of interest here ($T = 1 - 300°K$) were found to be insensitive to the form of the short-range potentials and the choice of R_0 as well. Thus we omit the details of our analytic fits in this region. At $R = R_0$, we join the short-range potentials smoothly onto long-range forms. Thus,

$$V_-(R) = \alpha R^2 e^{-\beta R} - C/R^6,$$

$$V_+(R) = V_-(R) + \gamma e^{-\tau R}, \quad R \geq R_0 = 6a_0, \qquad (14)$$

where the parameters α, β, and C may be assigned values consistent with the existing theoretical potentials, or they may be varied over a range of values; we have followed both procedures. The parameters γ and τ are chosen to reproduce the difference $V_+(R) - V_-(R)$ in the region $R = 5$ to $6a_0$, using the five-term results[3] for $V_+(R)$, but assuming the $V_+(R)$ and $V_-(R)$ curves do not cross. The total and diffusion cross sections are found to be insensitive to the choice of γ and τ. For purposes of comparison, we have also considered γ and τ appropriate to the original results of Buckingham and Dalgarno. Parameters representing the potentials of Matsen and co-workers and Buckingham and Dalgarno are given in Table I.

The van der Waals term $-C/R^6$ in Eqs. (14) causes the potentials to become attractive for large separations where dispersion forces are dominant. Dalgarno and Kingston have theoretically obtained the value $C \cong 29$ a.u.[14] However, since the $-C/R^6$ term in Eqs. (14) has the somewhat more general role of representing all of the attractive contribution to the potential for $R > R_0$, the parameter C appropriate to Eqs. (14) might be expected to be somewhat less than the correct van der Waals constant. In any case, we find that the inclusion of the attractive term in the potentials is important only for the lowest energies of consideration ($T < 4°K$), and therefore we take $C = 0$ throughout most of the investigation.

We have calculated cross sections for a variety of long-range potentials corresponding to different choices of parameters α, β in Eqs. (14). Rather than vary α explicitly, it was found convenient to vary the value of $V_-(R)$ at $R_0 = 6a_0$. Thus specifying $V_-(6a_0)$ and β, we have

$$\alpha = R_0^{-2} V_-(R_0) + C R_0^{-6} e^{\beta R_0},$$

where R_0 is taken to be $6a_0$. In Fig. 5 are plotted diffusion cross sections $Q_D(k)$ versus $k^2 (E = 0.0037k^2$ eV), calculated using the following potential curves: (1) Matsen and co-workers (see Table I), (2) Buckingham and Dalgarno (see Table I) with $C = 0$, (3) Buckingham and Dalgarno with $C = 20$, and (4) with $C = 30$. Curves 5-7 correspond to $V_-(6a_0) = 0.002$ a.u., $C = 0$ and $\beta = 1.4$, 1.6, and $1.8a_0^{-1}$, respectively. In order to illustrate the range of energies contributing to the average diffusion cross section at various temperatures, the distribution function of Eq. (2) is included for $T = 1$ and 300°K.

TABLE I. Parameters used in conjunction with Eq. (14) for representing the theoretical predictions of Buckingham and Dalgarno and Matsen and co-workers of the He(2^3S_1)-He(1^1S_0) interaction for internuclear separations greater than $6a_0$.

	Buckingham and Dalgarno[1]	Matsen and co-workers[a]
α	0.0712	0.0198
β	1.125	0.89
C	0, 20, 30	0.0
γ	10.307	1.54
τ	1.73	1.43

[a] Interaction potentials calculated by Greenawalt and Matsen and Matsen and Scott: as adjusted by Klein, Greenawalt, and Matsen (Refs. 2-4).

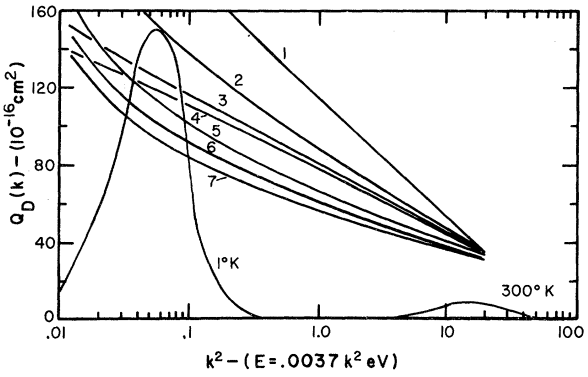

FIG. 5. Calculated diffusion cross sections $Q_D(k)$ vs k^2 in atomic units ($E=0.0037k^2$ eV). Curve 1 results from the potentials of Matsen *et al.*, and curves 2–4 from the potentials of Buckingham and Dalgarno with van der Waals coefficient $C=0$, 20, and 30 a.u., respectively. Curves 5–7 result from the parametrized potentials [Eqs. (14)] with parameter values of $V_-(6a_0)=0.002$ a.u., $C=0$ and $\beta=1.4$, 1.6, and $1.8a_0^{-1}$, respectively. Also shown is the distribution function of Eq. (2) for $T=1$ and 300° K.

V. COMPARISON BETWEEN MEASURED AND CALCULATED CROSS SECTIONS

The measured values of $\bar{Q}_D(T)$ over the temperature range 1–300°K are compared in Fig. 6 with the calculated cross sections, averaged according to Eq. (2). The cross sections, calculated with the potentials of Matsen and co-workers (1) or Buckingham and Dalgarano with $C=0$ (2) and $C=30$ (3), are all seen to be considerably larger than the measured values for all temperatures, indicating that these potentials are too large for $R\gtrsim 6a_0$. By varying the parameters $V_-(6a_0)$ and β with $C=0$, we were able to obtain long-range potentials yielding diffusion cross sections in good agreement with the measurements. The three curves 4*a*, 5, and 6 in Fig. 6, correspond to $V_-(6a_0)=0.002$ a.u., $C=0$, and $\beta=1.4$, 1.6, and $1.8a_0^{-1}$, respectively. The agreement is seen to be quite good for the $\beta=1.6$ curve, except possibly for the low-temperature region, where the calculated cross section appears to rise too steeply with decreasing energy. This indicates that for $C=0$, the potentials in Eqs. (14) are falling off too slowly for large values of R and suggests that the attractive $-C/R^6$ term should be included. Cross sections have been calculated for several choices of C; the dashed curves 4*b* and 4*c* are representative of the results and correspond to $V_-(6a_0)=0.002$ a.u., $\beta=1.4a_0^{-1}$ with $C=20$, and 30 a.u. respectively. The sensitivity of Q_D to C is of course greatest for low energies. As C is increased from 0 to 20 a.u., the low-energy diffusion cross sections are lowered, resulting in an improved agreement with the measured values. As C is further increased to 30 a.u. the attractive part of the potentials begins to dominate and the trend reverses, the cross sections becoming quite large. This behavior is easily understood since for $C=30$ a.u., the attractive part of the potentials is sufficiently strong to support a bound state.

An approximate analysis, based on the model of a hard sphere of radius r joined to an outer attractive part $-C/R^6$, yields a criterion for the existence of a bound state

$$C/r^4 \geq 0.003 \text{ a.u.}$$

Here r is taken to be the point where the V_- potential passes through zero; i.e., r is defined by

$$\alpha r^2 e^{-\beta r} - Cr^{-6} = 0.$$

For the case $V_-(6a_0)=0.002$ a.u. and $\beta=1.4a_0^{-1}$, a bound state is found to exist for $C=30$ but not for $C=20$. An analysis of the very low-energy *s*-wave phase shifts supports this. We are not in a position to rule out the possible existence of a bound state for the correct interaction potentials. However, using Eqs. (14) to represent the potentials $V_\pm(R)$, best agreement with the measurements is obtained for values of $C\cong 20$ a.u. This, does not imply that the value of 29 a.u. given by Dalgarno and Kingston is necessarily incorrect. The parameters C in our representation of the potentials could only be expected to agree in

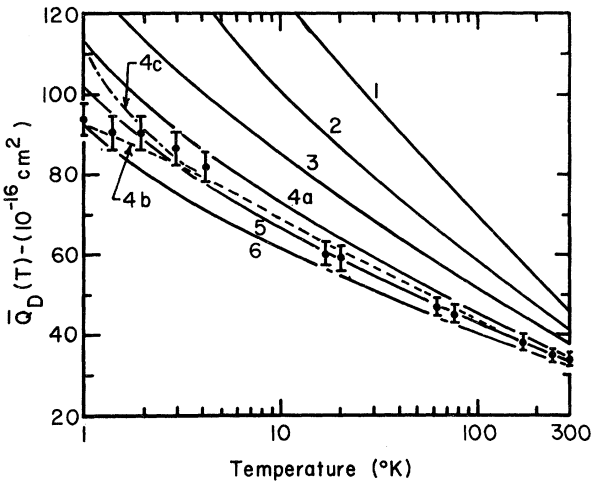

FIG. 6. Comparison between measured and calculated diffusion cross sections $\bar{Q}_D(T)$ in cm^2 versus temperature. Curve 1 results from the potentials of Matsen *et al*, curves 2 and 3 from the potentials of Buckingham and Dalgarno with van der Waals coefficient $C=0$ and 30 a.u., respectively. Curves 4a, 5, and 6 result from the potentials [Eqs. (14)] with parameter values $V_-(6a_0)=0.002$ a.u., $C=0$ and $\beta=1.4$, 1.6, and $1.8a_0^{-1}$, respectively. The dashed curves 4b and 4c correspond to the $V_-(6a_0)=0.002$ a.u., $\beta=1.4a_0^{-1}$ potentials with $C=20$ and 20 a.u., respectively. A comparison of curves 4a and 4b indicates that the additional van der Waals term tends to decrease the low-temperature diffusion cross sections; however, as C is increased further the weak van der Waals potential well (potential minimum at roughly $11a_0$) can support a bound state and the low-temperature diffusion cross sections become very large as shown by curve 4c.

magnitude with the correct van der Waals constant if the scattering occurred from regions of R completely dominated by the dispersion interaction.

A unique determination of the interaction potentials by comparison between measured and calculated diffusion cross sections is clearly not possible. We have found a variety of choices for the parameters $V_-(6a_0)$, β, and C which yield reasonable results. In Fig. 7 the acceptable V_- potentials are represented in the region $6a_0 \leq R \leq 11a_0$ by the hatched area; curves 1 and 2 correspond $V_- 6a_0)$ = 0.002 a.u., $C=0$, $\beta=1.6$, and $V_-(6a_0)=0.002$, $C=20$, and $\beta=1.4$, respectively. Also given for comparison are the V_- potentials of Matsen and Scott (curve 3) and Buckingham and Dalgarno with $C=0$ (curve 4) and $C=30$ a.u. (curve 5) all of which appear to be considerably too large in this long-range region.

Having determined potentials consistent with the diffusion data, we proceeded to calculate total and excitation transfer cross sections to compare with other measurements. Total cross sections for $He(2^3S_1)$-$He(1^1S_0)$ scattering in the relative velocity range of 1000 to 3000 m/sec have been measured by Rothe, Neynaber, and Trujillo using a beam-gas attenuation method.[15] They suggest the error in the measurements to be less than 10%. These experimental measurements are compared in Fig. 8 with total cross sections calculated using the potentials $V_-(6a_0)=0.002$ a.u., $\beta=1.4$,

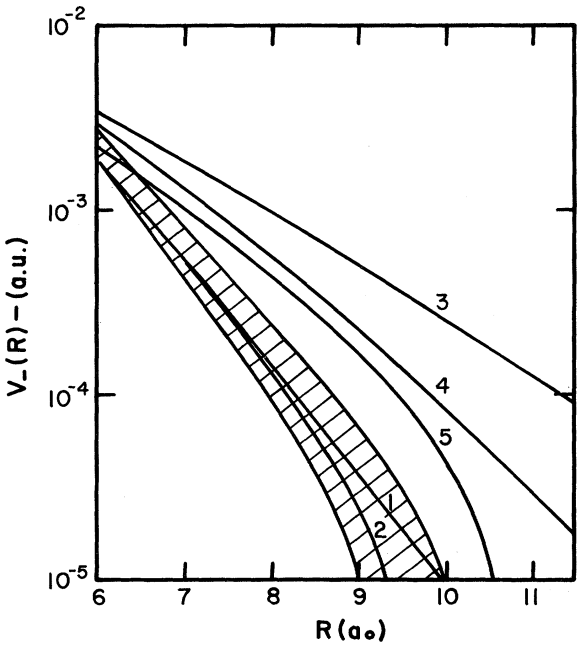

FIG. 7. Long-range $He(2^3S_1)$-$He(1^1S_0)$ interaction potentials in atomic units (1 a.u. = 27.2 eV) which yield the cross sections shown in Figs. 5, 6, 8, and 9. Hatched area designates range of acceptable V_- potentials. Curves 1 and 2 correspond to the potentials $V_-(6a_0)=0.002$; $C=0$, $\beta=1.6a_0^{-1}$ and $C=20$ a.u., and $\beta=1.4a_0^{-1}$, respectively. Curves 3–5 correspond to the potentials of Matsen *et al.*, and Buckingham and Dalgarno $C=0$ and $C=30$ a.u., respectively.

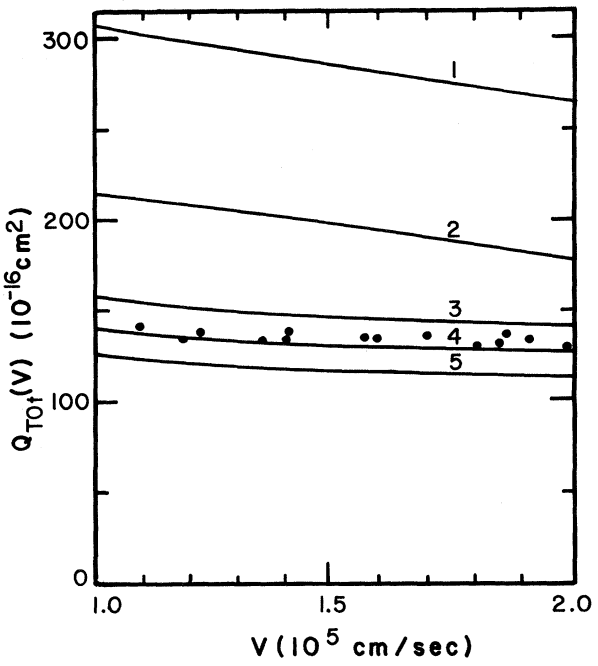

FIG. 8. $He(2^3S_1)$-$He(1^1S_0)$ total scattering cross section versus relative velocity. Curves 1 and 2 result from the potentials of Matsen *et al.*, and Buckingham and Dalgarno, curves 3–5 from the potentials $V_-(6a_0)$ = 0.002 a.u., $C=0$ and $\beta=1.4$, 1.6, and $1.8a_0^{-1}$ respectively. Experimental data taken from Rothe, Neynaber, and Trujillo (Ref. 15).

1.6, and $1.8a_0^{-1}$ and $C=0$. Again $\beta=1.6a_0^{-1}$ is the best choice with $\beta=1.4$ and $1.8a_0^{-1}$ bracketing the experimental uncertainties. Included for comparison are total cross sections calculated using the potentials of Buckingham and Dalgarno and Matsen and Scott.

The excitation-transfer cross section, defined in Eq. (11), is particularly interesting because of its sensitivity to the difference in the potentials, $V_+(R)-V_-(R)$, as well as to the potentials themselves. This difference is represented by $\gamma \exp(-\tau R)$ and, as discussed previously, the parameters γ and τ were chosen from the available theoretical determinations of the $^3\Sigma_g^+$ and $^3\Sigma_u^+$ energies. Thus a comparison between the calculated excitation-transfer cross sections and the observed values provides a consistency check on the potentials previously determined from the diffusion data, and on the magnitude of the difference between the potentials. In Fig. 9 the averaged product of relative velocity and metastability exchange cross section obtained by Colegrove, Schearer, and Walters[5] in a He^3 optical pumping experiment is compared with our calculations using the three potentials $V_-(6a_0)$ = 0.002 a.u., $C=0$ with $\beta=1.4$ (1), 1.6 (2), and $1.8a_0$ (3). As before, the $\beta=1.6a_0^{-1}$ curve is found to be in best agreement.

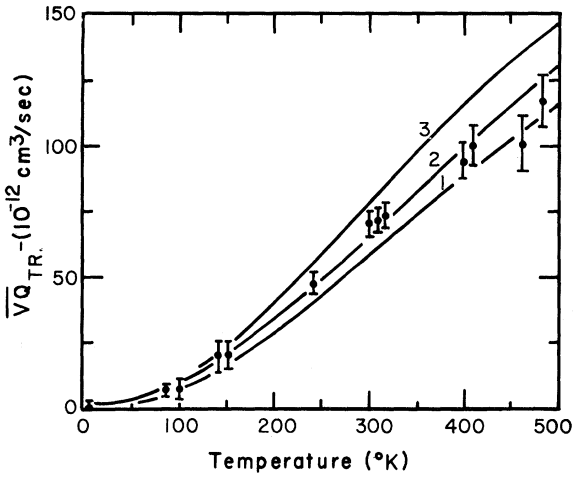

FIG. 9. $He(2^3S_1)$-$He(1^1S_0)$ metastability exchange rate versus temperature. Curves 1–3 result from the potentials $V_-(6a_0) = 0.002$ a.u., $C = 0$ and $\beta = 1.4$, 1.6, and $1.8a_0^{-1}$, respectively. Experimental data taken from Colegrove, Schearer, and Walters (Ref. 5).

SUMMARY

The principal results of this study can be summarized as follows:

(a) The diffusion coefficient for $He(2^3S_1)$ atoms in helium gas has been measured over the temperature range from 1 to 300°K. The thermally averaged diffusion cross sections extracted by means of Chapman-Enskog theory are 82, 58, 46, and 34 (10^{-16} cm^2) at 4.2, 20, 77, and 300°K, respectively. The estimated uncertainty is ±5% at all temperatures.

(b) Averaged diffusion cross sections calculated from available theoretical 2^3S_1-1^1S_0 helium interaction potentials are much larger than the experimental cross sections, suggesting that the long-range repulsion has been overestimated.

(c) The interaction potentials were therefore parametrized in a manner consistent with the existing theory of the interaction, and the parameters were varied until good agreement was obtained between measured and computed diffusion cross sections. The interaction potentials so obtained exhibit long-range repulsive interactions that are substantially weaker than predicted by available theories.

(d) The best-fit parametrized potentials were then used without further adjustment to calculate 2^3S_1-2^1S_0 total and excitation transfer cross sections, and the results are in excellent agreement with previous, independent, experimental values.

---

*Work supported in part by the U. S. Atomic Energy Commission. Based on part of a Ph. D. thesis submitted by W. A. Fitzsimmons to Rice University, 1968.

†Alfred P. Sloan Foundation Fellow.

[1]R. A. Buckingham and A. Dalgarno, Proc. Roy. Soc. (London) A213, 327 (1952).

[2]F. A. Matsen and D. R. Scott, in Quantum Theory of Atoms, Molecules, and the Solid State, edited by Per-Olav Löwdin (Academic Press, Inc., New York, 1966).

[3]E. M. Greenawalt, Ph. D. thesis, University of Texas (to be published).

[4]D. J. Klein, E. M. Greenawalt, and F. A. Matsen, J. Chem. Phys. 47, 4820 (1967).

[5]F. D. Colegrove, L. D. Schearer, and G. K. Walters, Phys. Rev. 135, A353 (1964).

[6]R. A. Buckingham and A. Dalgarno, Proc. Roy. Soc. (London) A213, 506 (1952).

[7]A. V. Phelps, Phys. Rev. 99, 1307 (1955).

[8]A. O. McCoubrey, Phys. Rev. 93, 1249 (1954).

[9]I. Ya. Fugol' and P. L. Pakhomov, Zh. Eksperim. i Teor Fiz. Pis'ma Redakt. 3, 389 (1966) [English transl: JETP Letters 3, 254 (1966)].

[10]S. Chapman and T. G. Cowling, The Mathematical Theory of Nonuniform Gases (Cambridge University Press, Cambridge, England, 1952), 2nd ed.

[11]H. S. W. Massey and R. A. Smith, Proc. Roy. Soc. (London) A142, 142 (1933).

[12]N. F. Mott and H. S. W. Massey, The Theory of Atomic Collisions (Oxford University Press, Oxford, England, 1955), 3rd ed.

[13]B. K. Gupta, private communication.

[14]A. Dalgarno and A. E. Kingston, Proc. Phys. Soc. (London) 72, 1053 (1958).

[15]E. W. Rothe, R. H. Neynaber, and S. M. Trujillo, J. Chem. Phys. 42, 3310 (1965).